CrossMark

Ultrafast all-optical ALU operation using a soliton control within the cascaded *InGaAsP/InP* microring circuits

S. Soysouvanh[1] · P. Phongsanam[2] · S. Mitatha[1] · J. Ali[3] · P. Yupapin[4,5] · I. S. Amiri[6] · K. T. V. Grattan[7] ·
M. Yoshida[8]

Abstract

A dark-bright soliton conversion is used to perform the two arithmetic logic unit operations namely adder and subtractor operations. The advantage of the system such as power stability, non-dispersion and the dark-bright soliton phase conversion control can be obtained. The input source into the circuit is the bright soliton pulse, with the pulse width of 35 ps, the peak power at 1.55 μm is 1 mW. By using the dark-bright soliton conversion pair, the generated logic bits can be controlled, and the secure bits can be achieved. The simulation results show the output signal with a minimum loss of only 0.1% with respect to a low input power of 1 mW, and ultra-fast response time of about 1 ps can be achieved. It gives the ultra-high bandwidth of more than 40 Gbits^{-1}. The circuit composes six microring resonators made of *InGaAsP/InP* material with smaller ring radii of 1.5 μm, and the total physical scale of the circuit less than 100 μm^2.

1 Introduction

By reason of the rapid improvements in optical or photonic computing for higher computation, processing speeds and minimal transmission losses are desirable. For decades, most research and investigation is on replacing current computer component redundancy with the equipment, resulting in the optical digital computing systems for processing optical binary data (Kumar et al. 2015; Tian et al. 2015; Godbole et al. 2016; Mehdizadeh and Alipour-Banaei 2017). All-optical adders are important elements in any all-optical arithmetic and logical units, many researchers have demonstrated various techniques to

perform all-optical arithmetic and logical operations (Garai 2011; Gayen et al. 2012; Chattopadhyay 2012; Stanley et al. 2015; Kaur et al. 2015; Theresal et al. 2015). Furthermore, the increasing demand on miniaturizing quantum computers requires an improvement in power consumption. However, most of the previous works need the use of optoelectronic devices in which 30% loss in electro-optic conversion is observed in addition to the decrease in transmission speed. However, such problems are overcome by the use of another form of the input data source, which is known as the optical soliton pulse (Raj et al. 2014; Amiri et al. 2017) propagating within nonlinear material i.e., InGaAsP/InP (Seifert and Runge 2016). It can provide

✉ P. Yupapin
preecha.yupapin@tdt.edu.vn

1 Department of Computer Engineering, Faculty of Engineering, King Mongkut's Institute of Technology Ladkrabang, Bangkok 10520, Thailand

2 Faculty of Engineering, Kasem Bundit University, 1761 Phatthanakan Rd, Suan Luang, Bangkok 10250, Thailand

3 Laser Center, IbnuSina Institute for Industrial and Scientific Research, Universiti Teknologi Malaysia (UTM), Skudai, Malaysia

4 Computational Optics Research Group, Advanced Institute of Materials Science, Ton Duc Thang University, District 7, Ho Chi Minh City 700000, Vietnam

5 Faculty of Electrical & Electronics Engineering, Ton Duc Thang University, District 7, Ho Chi Minh City 700000, Vietnam

6 Division of Materials Science and Engineering, Boston University, Boston, MA 02215, USA

7 Department of Electrical and Electronic Engineering, School of Mathematics, Computer Science and Engineering, The City, University of London, London EC1V 0HB, UK

8 Department of Embedded Technology, School of Information and Telecommunication Engineering, Tokai University, 2-3-23, Takanawa, Minato-ku, Tokyo 108-8619, Japan

🖄 Springer

optical–electrical–optical (OEO) conversions, thus lessening the need for electrical power and reduce the transmission loss. This paper presents a 1-bit all-optical full-adder and subtractor circuit which can be used to design 1-bit all-optical arithmetic unit (AU) to perform 4 arithmetic operations i.e. addition, subtraction, increment and decrement based on microring resonator device with a scale of 1.5 μm radius (Xu et al. 2008), which has been fabricated and demonstrated in various applications (Thongmee and Yupapin 2011; Madani et al. 2013; Yan et al. 2014; Donzella et al. 2015; Kumar 2016). The design circuit can offer the advantage of dark-bright soliton conversion control technique within the ring resonator (Teeka et al. 2009, 2010), in which the optical logic "0" and logic "1" are represented by optical dark soliton "D" and bright soliton "B" pulses, respectively. In this paper, the advantage of the dark-bright soliton conversion signal is employed, from which the generated codes can be used for security purpose. In addition, the ultrafast switching of the soliton pulse property can speed up the process of code generation. The combination of the bit operation is obtained by the cascaded mirroring circuits, which are six GaAsInP/P microring devices in the design. Simulations show that the proposed full-adder and full subtractor achieved high-speed operation with and small time-delay compared to other 1-bit conventional adders (Dai et al. 2013; Gayen and Chattopadhyay 2013), and the experimental results of ring resonator (Wang et al. 2016) show high-quality factors (Q), free spectral range (FSR), obtainable from ring resonator.

2 Operating principle

An arithmetic unit (AU) is a combinational circuit integrated into an arithmetic logic unit (ALU) that performs arithmetic operations on integer binary numbers. This is in contrast to an (FPU), which operates on floating point numbers. An AU is a fundamental building block of many types of computing circuits, including the central processing unit (CPU) of computers, the floating-point unit (FPUs), and graphics processing units (GPUs). A single CPU, FPU or GPU may contain multiple ALUs. The addition and subtraction are the basis for many important operations such as address generation, multiplication, division which are commonly used in ALUs. In the 1-bit arithmetic unit with two selected inputs can perform 4 arithmetic operations such as addition, subtraction, increment and decrement based on a full-adder circuit. Several designs of adders have been proposed. In Dai et al. (2013), all-optical half-adder using Terahertz optical asymmetric demultiplexer (TOAD) switch is proposed. The proposed model is attractive since no additional input beam is used

in a half-adder unit and also the numerical simulation is done at 11.11 Gbps in order to investigate the suitable operating condition. However, due to their slow processing speed is quite low compared to other state-of-art designs. In Gayen and Chattopadhyay (2013), the authors show a new and potentially integrable scheme for the realization of an all-optical binary full adder, using a Mach–Zehnder interferometer (MZI) based on a semiconductor optical amplifier (SOA). The designed system has a successful operation of at 10 Gb/s with return-to-zero modulated signals. But due to a lot of circuit elements may result in the large physical size of the full adder, which inhibits integration. Therefore, in this paper present the new technique that can implement the logic operation with ultra-fast switching time, and can reduce the physical size of the overall system, which is useful for further photonic integration. In our previous work (Thongmee and Yupapin 2011) shows the illustration of the dark-bright soliton conversion signal that can form an all-optical half-adder which is very simple and flexible system. In operation, an optical channel dropping filter (OCDF) based microring resonator (MRR) is made up of two straight waveguides coupled with a ring-type waveguide, which is given in the following section. Here Fig. 1a is represented by Fig. 1b for consistency.

The coupling equation outlined in the Rakshit et al. (2013, 2014) demonstrates a relative phase of between the input signal at the input port and the signal coupled into the ring. Likewise, the signal coupled into the drop and through ports, where both are acquired a phase of $\pi/2$ regarding the signal in the input port. From Fig. 2, we can obtain the electrical fields of MRR as following equations.

$$E_{ra} = -j\kappa_1 E_{in} + \tau_1 E_{rb} \exp\left(\frac{j\omega T}{2}\right) \exp\left(\frac{-\alpha L}{4}\right) \quad (1)$$

$$E_{rb} = j\kappa_2 E_{ad} + \tau_2 E_{ra} \exp\left(\frac{j\omega T}{2}\right) \exp\left(\frac{-\alpha L}{4}\right) \quad (2)$$

$$E_{th} = \tau_1 E_{in} - j\kappa_1 E_{rb} \exp\left(\frac{j\omega T}{2}\right) \exp\left(\frac{-\alpha L}{4}\right) \quad (3)$$

$$E_{dr} = \tau_2 E_{ad} - j\kappa_2 E_{ra} \exp\left(\frac{j\omega T}{2}\right) \exp\left(\frac{-\alpha L}{4}\right) \quad (4)$$

where E_{in} is the input electric field, E_{ad} is the add (control) electric field, E_{th} is the output electric field at through port, E_{dr} is the output electric field at drop port, E_{ra} and E_{rb} are the electric fields circulating inside the ring at point a and b, respectively. κ_1 is the field coupling coefficient between the input and the ring, κ_2 is the field coupling coefficient between the ring and the output bus, L is the circumference of the ring ($L = 2\pi R$), here R is the radius of the ring measured from the center of the ring to the center of the waveguide. T is the field propagation time taken for one roundtrip inside the ring ($T = Ln_{eff}/c$), and α is the power
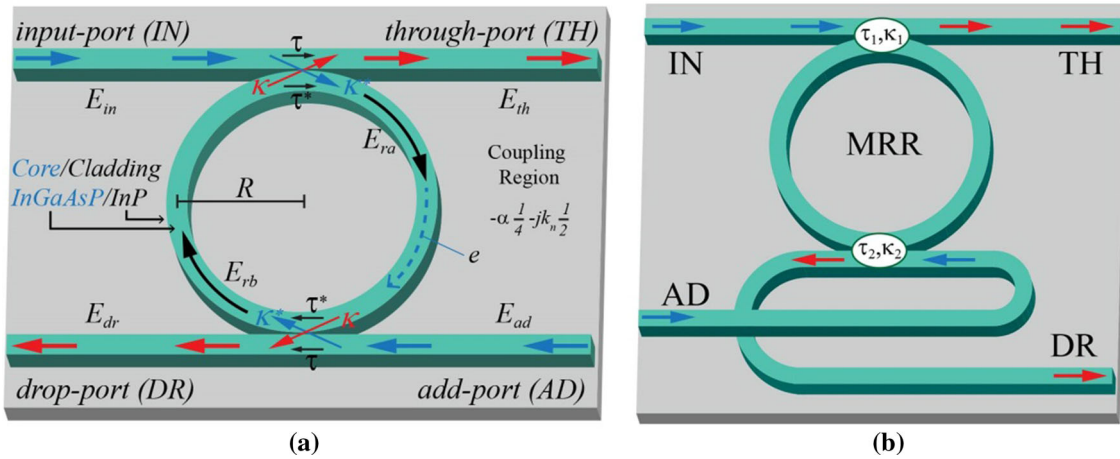
Fig. 1 A schematic of a micro-ring resonator (MRR) system, where E_{in}, E_{th}, E_{dr} and E_{add} are the optical field at the input, through and drop ports, respectively. IN, TH, DR and AD are the microring circuit at the input, through and drop ports, respectively

loss in the ring per unit length. We assume that lossless coupling, i.e. $\tau_{1,2} = \sqrt{1 - \kappa_{1,2}^2}$. The transfer function of output power/intensities at through port and drop port is given by (5) and (6), respectively.

$$|E_{th}|^2 = \left| \frac{\tau_2 - \tau_1 A\Phi}{1 - \tau_1\tau_2 A\Phi} E_{in} + \frac{-\kappa_1\kappa_2 A_{1/2}\Phi_{1/2}}{1 - \tau_1\tau_2 A\Phi} E_{ad} \right|^2 \quad (5)$$

$$|E_{dr}|^2 = \left| \frac{\tau_2 - \tau_1 A\Phi}{1 - \tau_1\tau_2 A\Phi} E_{ad} + \frac{-\kappa_1\kappa_2 A_{1/2}\Phi_{1/2}}{1 - \tau_1\tau_2 A\Phi} E_{in} \right|^2 \quad (6)$$

where $A_{1/2} = \exp(-\alpha L/4)$ is the half-roundtrip amplitude ($A = A_{1/2}^2$), $\Phi_{1/2} = \exp(j\omega T/2)$ is the half-roundtrip phase contribution ($\Phi = \Phi_{1/2}^2$). $\tau_{1,2} = \sqrt{1 - \kappa_{1,2}^2}$, κ_1 and κ_2 are the coupling constants.
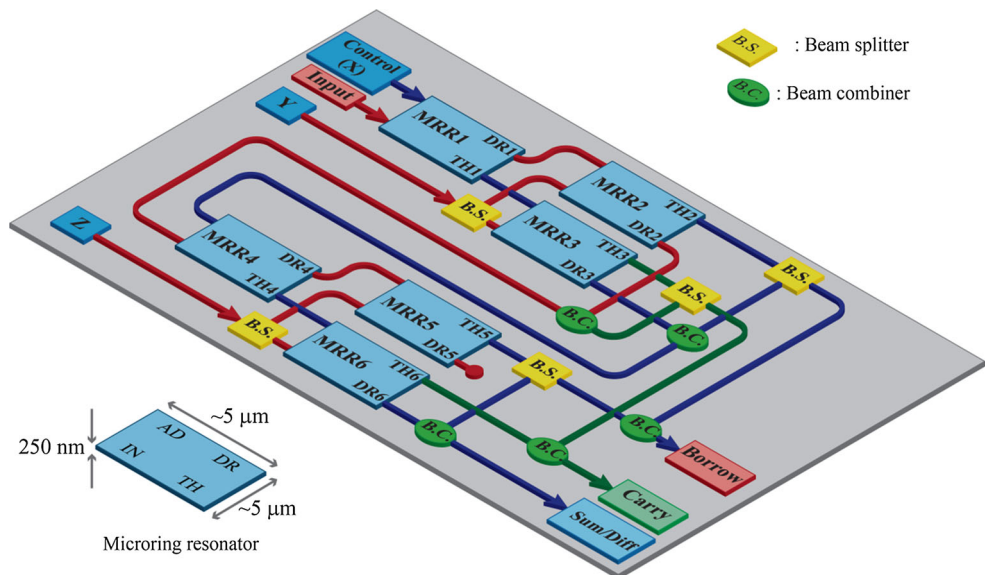
The input and control electric fields at the input port and drop port are formed by optical dark soliton ($E_{in(D)}$) and bright soliton ($E_{in(B)}$) as given in (7) and (8), respectively.

$$E_{in(D)}(t) = A_0 \tanh\left[\frac{T}{T_0}\right] \exp\left[\left(\frac{z}{2L_D}\right) - i\omega_0 t\right] \quad (7)$$

$$E_{in(B)}(t) = A_0 \text{sech}\left[\frac{T}{T_0}\right] \exp\left[\left(\frac{z}{2L_D}\right) - i\omega_0 t\right] \quad (8)$$

where A is the optical field amplitude and z is the propagation distance. T is the soliton propagation time in the frame moving at the group velocity ($T = t - \beta_1 z$), here β_1 and β_2 are the coefficients of the linear and second-order terms of Taylor expansion of the propagation constant. L_d is the dispersion length of the soliton pulse ($L_d = T_0^2/\beta$). T_0 is the initial soliton pulse width, where t is the soliton phase shift time, and ω_0 is the frequency of the soliton.

Fig. 2 A schematic of the designed circuit for all-optical ALU circuit, where Y and Z: the input soliton pulse, MRR: microring circuit, IN, TH, DR and AD are the microring circuit at the input, through, drop and add ports, respectively

The above solutions describe a pulse that keeps its temporal width invariance as it propagates and thus is called a temporal soliton. When a soliton peak intensity is $(\beta/\Gamma T_0^2)$, then T_0 is known. In case of the soliton pulse in the micro (or nano) ring device is applied, a balance length should be achieved between dispersion length (L_d), where the nonlinear length is ($L_{nl} = 1/\Gamma\phi_{nl}$), where Γ is the length scale over which dispersive or nonlinear effects make the beam become wider or narrower ($\Gamma = n_2k_0$). There is a balance between dispersion and nonlinear lengths, hence, $L_d = L_{nl}$. When light propagates within the nonlinear material (medium), the refractive index (n) of light within the medium is given by $n = n_0 + n_2I = n_0 + n_2(P/A_{eff})$, where n_0 and n_2 are the linear and nonlinear refractive indexes, respectively. I is the optical intensity and P is the optical power. A_{eff} is the effective mode core area of the device. For micro/nano ring resonator, the effective mode core areas range from 0.1 to 0.5 μm^2 (Thongmee and Yupapin 2011). The resonant output of the light field is the ratio between the output field ($E_{out}(t)$) and input field ($E_{in}(t)$) in each roundtrip.

3 Design of all-optical ALU

In order to design the all-optical circuit of the arithmetic logic unit (ALU) for operating two arithmetic operations i.e., full-addition (FA) and full-subtraction (FS) with three binary inputs (XYZ), we relied on the truth table of binary arithmetic operation as illustrated in Table 1, where we can get simplified Boolean's equations obtained as a sum of product for each output as shown in Table 1, we can design an ALU circuit for performing FA and FS by combining the summation of FA (*Sum*) and difference of FS (*Diff*) together as illustrated in Fig. 2. In the design, a circuit consists of 6 microring resonator (MRRs), 5 beam splitters (B.S.) and 5 beam combiners (B.C.). Here the approximate physical size of the MRR is 6 μm wide, 8 μm long, 250 nm thick, has 290–440 nm of waveguide width and $\sim$ 1.5 μm of ring radius (Xu et al. 2008). The proposed scheme of all-optical ALU is shown in Fig. 2. Initially when the input pulse train and control pulse is input into the first microring (MRR1) using dark soliton (logic 0) or bright soliton (logic 1), then the optical soliton is converted to be dark and bright via MRR1 which can be seen at the through port and drop port with π phase shift (Hwang et al. 2007), and MRR1 then functions as an inverter gate like. Hence, the outputs of MRR1 can be written as TH1 = $\overline{X}$ and DR1 = X. Subsequently, the output signals from MRR1 are applied into input-ports of MRR2 and MRR3. Next, the input data "Y" with logic "0" (Dark) or logic "1" (Bright) are added into both add-ports and then the dark-bright

soliton conversion with π phase shift is operated again by using MRR2 and MRR3. The results obtained are simultaneously seen at the output ports of MRR2 and MRR3 for optical logic operation and can be written as TH2 = $\overline{X}Y$, DR2 = $\overline{XY}$, TH3 = XY, DR3 = $X\overline{Y}$ which can be used to perform half-addition (HA) and half-subtraction (HS) as $S_{HA} = D_{HS} = \overline{X}Y + X\overline{Y}$, $C_{HA} = XY$, and $B_{HS} = \overline{X}Y$. To operate the all-optical HA and HS (Thongmee and Yupapin 2011) can be easily done by using beam splitters (B.S) and beam combiners (B.C) e.g., a fiber coupler or optical Y-branch. The beam splitters used in the system are not polarizing. The ratio of reflection-transmission is 50:50 (or 50%) for all polarizations of the incident light. Then the operation of full-adder (FA) and full-subtractor (FS) can be performed by using MRR4, both input signals are generated by the first HA state (S_{HA}), then the dark-bright soliton conversion is operated again and generate the output at output-port TH4 = SHA, DR4 = $\overline{S_{HA}}$. Both output signals are applied to be the input signals of MRR5 and MRR6, respectively. This state, an optical input pulse "Z" with logic "0" or logic "1" is input into both add-ports (MRR5 and MRR6) then the last operation of dark-bright conversion is done again by MRR5 and MRR6. The results are obtained simultaneously at output-ports as TH5 = $\overline{S_{HA}}Z$, DR-5 = $\overline{S_{HA}}\overline{Z}$, TH6 = $S_{HA}Z$ and DR6 = $S_{HA}\overline{Z}$.

Finally, the full-addition/subtraction is done by combining the optical signal from output-ports of MRR2, MRR3, MRR5 and MRR6, where the full-addition and full-subtraction are expressed by Eqs. (9)–(12) (Fig. 3).

$$Sum = \overline{S_{HA}}Z + S_{HA}\overline{Z} = TH5 + DR6 \qquad (9)$$

$$Carry = XY + S_{HA}Z = TH3 + TH6 \qquad (10)$$

$$Difference = \overline{D_{HS}}Z + D_{HS}\overline{Z} = TH5 + DR6 \qquad (11)$$

$$Borrow = \overline{X}Y + \overline{S_{HA}}Z = TH2 + TH5 \qquad (12)$$

Table 1 Truth table of binary arithmetic operation

Inputs			Addition		Subtraction	
X	Y	Z	Sum	Carry	Diff	Borrow
0	0	0	0	0	0	0
0	0	1	1	0	1	1
0	1	0	1	0	1	1
0	1	1	0	1	0	1
1	0	0	1	0	1	0
1	0	1	0	1	0	0
1	1	0	0	1	0	0
1	1	1	1	1	1	1

4 Simulation results

In a simulation, in order to perform optical switch with an optimum result, the parameters are fixed for all MRR as shown in Table 2. The input power for dark and bright soliton pulses is 1 mW, soliton pulses width is 35 ps and the center wavelength is $\lambda_0 = 1.55$ μm, and the ring radius is 1.55 μm. The transmission characteristic of MRR is as shown in Fig. 5, where the on–off ratio is 47.99 dB, the free spectral range (FSR) is 70 nm, and the full-width at half maximum (FWHM) is 7 nm. The suitable parameters used in our simulation in concluded in Table 2. Base on nonlinear optical effect cross-phase modulation (XPM) is applied in this mechanism in order to reduce or change the refractive index of MRR. The optical signals at through-port and drop-port can be controlled, which can perform the optical switching in InGaAsP/InP material based (Hwang et al. 2007; Mookherjea and Schneider 2008), and represented the logic NOT gate as illustrated in Fig. 4. The optical logic switching can be concluded that, when there is no control signal (the signal at add-port), the input signal will be transmitted to drop-port (DR). In another side, when the control signal is applied, then the refractive index of the waveguide is changed and causes the change of resonant wavelength, thus the input signal will be transmitted to through-port (TH). The operations of all-optical simultaneous full adder/subtractor are concluded in Table 3 and Fig. 5. Figure 5a shows the transmitted signal at output-ports of ALU circuit for the first case where control input "XYZ" is "000". Initially, the continuous input signal is input into MRR1 via the input port and there is no control signal (X = 0), hence the optical signal is
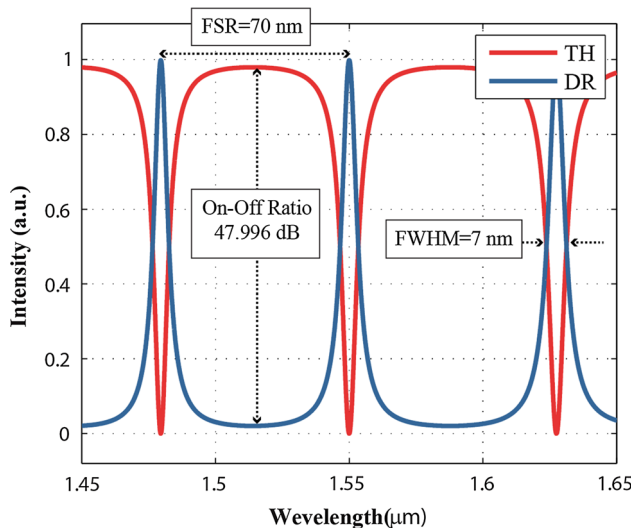

Fig. 3 Transmission characteristics of bright soliton pulse within the MRR when the ring radius is 1.55 μm, κ = 0.25, m = 21 and $\lambda_R = 1.55$ μm, where the dark-bright soliton pair is processed as the "On–Off" signals

transmitted drop-port (DR1) due to resonance condition. Subsequently, the optical signal from DR1 is input into MRR2 via an input port and there no control input (Y = 0) is applied to MRR2), therefore, the optical signal will be appeared at drop-port (DR2) to be optical logic "1". The optical signal from DR2 is then used to be input signal of MRR4 via input-port and appear at the drop-port (DR4) due to the resonance condition. The signal is then input into input-port of MRR5 and then no control input (Z = 0) is applied to MRR5, hence, the optical signal is again transmitted to drop-port (DR5) due to resonance condition and represents the optical logic "01000100" at output-ports "TH2-DR2-TH3-DR3-TH5-DR5-TH6-DR6", respectively. Figure 5b shows the transmitted signal when the input XYZ is "001", for in this case at the initial state is the same as the previous case where control input (XY = 00). Therefore, the input signal is transmitted to drop-ports (DR2 and DR4) and later on input into MRR5 via input-port. For this state, the control input is applied (Z = 1), thus, the optical signal is switched from drop-port (DR5) to through-port (TH5) and represents the optical logic "01001000" at output-ports "TH2-DR2-TH3-DR3-TH5-DR5-TH6-DR6". Figure 5c shows the output signal when the input XYZ is "010". This case, there is no control input (X = 0) is applied to MRR1, thus the input signal is transmitted into drop-port (DR1) again. Next, the signal from DR1 is input into MRR2 via input-port and control input (Y = 1) is applied to MRR2 via add-port, therefore, the optical signal is switched from drop-port (DR2) to through-port (TH2) as optical logic "1". The signal from TH2 is later on used as the input signal of MRR4 via add-port and appear at the through-port (TH4) due to the resonance condition, and then applied to MRR6 via input-port. For this state, control input (Z = 1) is applied to MRR6 via add-port, thus, the optical signal is transmitted to drop-port (DR6) and represents the optical logic "10000001" at output-ports "TH2-DR2-TH3-DR3-TH5-DR5-TH6-DR6".

Figure 5d shows the output when the input XYZ is "011". This case is the same as the previous case for the first and second states where (XY = 01), and the optical is transmitted to through-port (TH2) as optical logic "1". The signal from TH2 is then used to be input signal of MRR2 via add-port and appear at the through-port (TH4) due to the resonance condition and applied to MRR6. Where in this state, the control input is applied (Z = 0), thus, the optical signal is appeared at through-port (TH6) and represents the optical logic "10000010" at output-ports "TH2-DR2-TH3-DR3-TH5-DR5-TH6-DR6". Figure 5e shows the output when the input XYZ is "100". This case, the control pulse is applied to MRR1 (X = 1), thus the input signal is transmitted to through-port (TH1). Next, the signal from TH1 is input into MRR3 via input-port and

Table 2 Ring resonator parameters used in simulation for optimum outputs

Parameter variables	Explanation	Values
R	Radius of the ring waveguide (measured from the center of the ring to the center of the waveguide)	1.55 μm
W	Width of the waveguides	$\sim$ 290 to $\sim$ 440 nm
H	Height of the waveguides	250 nm
L	Circumference of the ring waveguide (optical path lengths in a ring)	9.74 μm
A_{eff}	Effective mode core area	0.25 μm^2
κ	Coupling coefficients	0.25
γ	Coupling loss	0.10 dB
α	Intensity attenuation loss inside the ring	0.50 dB/cm
n_{eff}	Effective refractive index of the ring (InGaAsP/InP)	3.34
Δn	Change of refractive index when control is applied (Bright soliton)	3.5×10^{-3}
λ_R	Resonance wavelength	1.55 μm
$\Delta \lambda_R$	Resonance wavelength after control is applied (Bright soliton)	1.54 μm

Fig. 4 Transmission signal at through-port (TH) and drop-port (DR) of MRR, when the peak output intensity represented to be logic "1" and the weak output intensity is represented to be logic "0", the secure signal can be obtained by the applying the control input signal
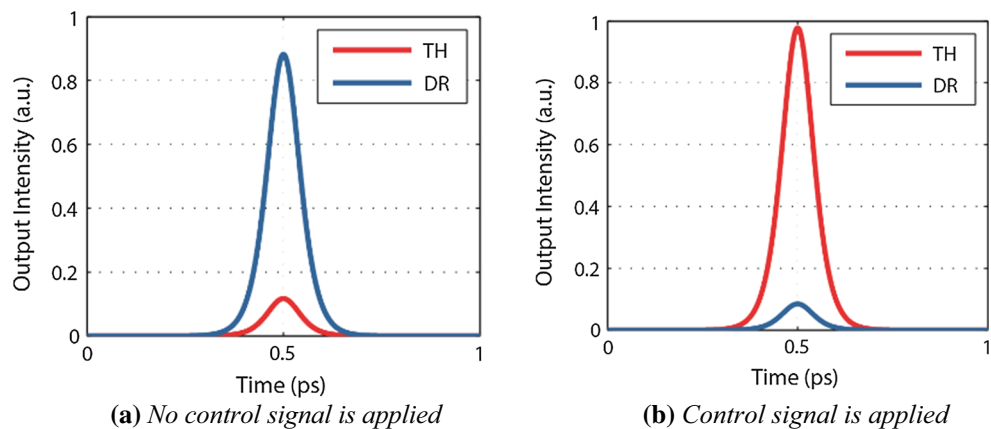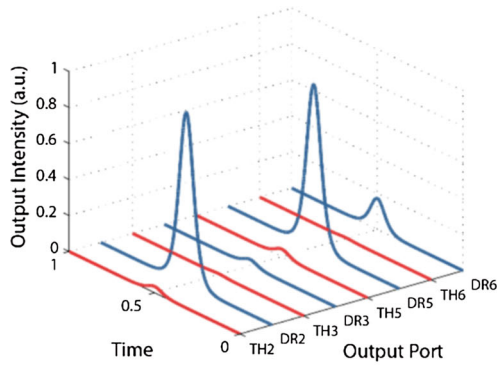

(a) *No control signal is applied*

(b) *Control signal is applied*

Table 3 Conclusion of all-optical full-adder/subtractor

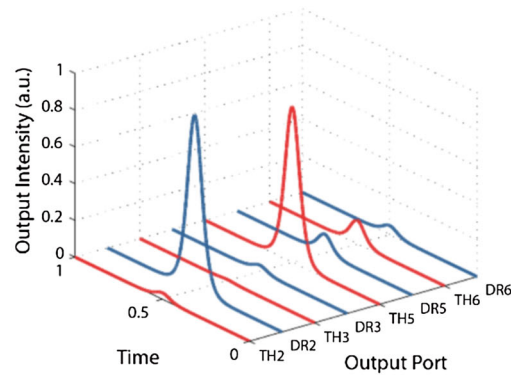| Inputs			Output ports								Results			
X	Y	Z	TH2	DR2	TH3	DR3	TH5	DR5	TH6	DR6	CAR	BOR	SUM	DIF
D	D	D	D	B	D	D	D	B	D	D	D	D	D	D
D	D	B	D	B	D	D	B	D	D	D	D	B	B	B
D	B	D	B	D	D	D	D	D	D	B	D	B	B	B
D	B	B	B	D	D	D	D	D	B	D	B	B	D	D
B	D	D	D	D	D	B	D	D	D	B	D	D	B	B
B	D	B	D	D	D	B	D	D	B	D	D	D	D	D
B	B	D	D	D	B	D	D	B	D	D	B	D	D	D
B	B	B	D	D	B	D	B	D	D	D	B	B	B	B

Logic "0" is Dark soliton (D); logic "1" is Bright soliton (B)

control input (Y = 1) is applied to add-ports (AD2), therefore, the optical signal is appeared at through-port (TH3) to be optical logic 1. The signal from TH3 is then used to be input signal of MRR4 via input-port and appear at the drop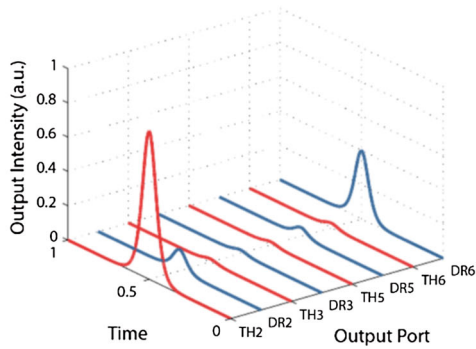-port (DR4) due to the resonance condition. The signal is then inputted into MRR6. For this state, no control input (Z = 0) is applied, thus, the optical signal is appeared at drop-port (DR6) and represents the optical logic "00010001" at output-ports "TH2-DR2-TH3-DR3-TH5-DR5-TH6-DR6". Figure 5f shows the output when the
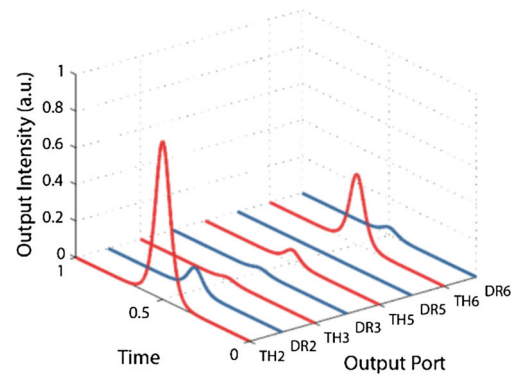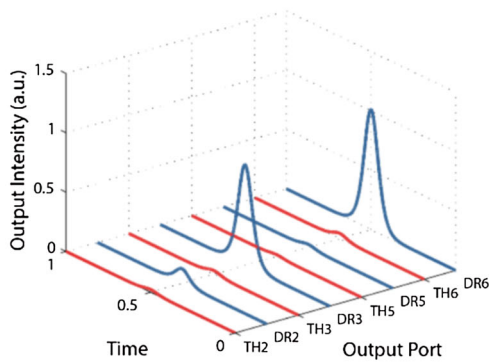
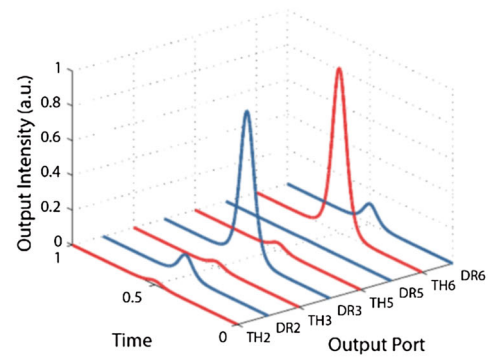**(a)** *output logic is "01000100"*

(b) *output logic is "01001000"*

(c) *output logic is "10000001"*

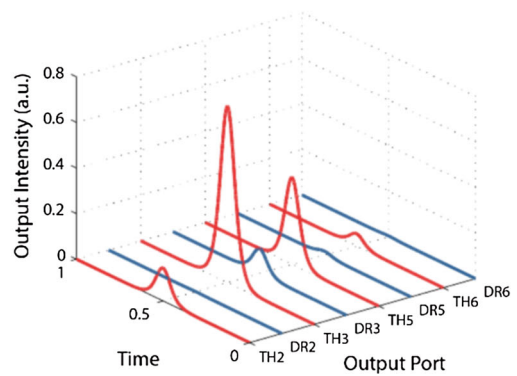**(d)** *output logic is "10000010"*

(e) *output logic is "00010001"*

(f) *output logic is "00010010"*

(g) *output logic is "00100100"*

(h) *output logic is "00101000"*

Fig. 5 Transmitted signals at output-ports of MRR2, MRR3, MRR5 and MRR6 when input logic "XYZ" is **a** "000", **b** "001", **c** "010", **d** "011", **e** "100", **f** "101", **g** "110", **h** "111"

input XYZ is "101". This case is the same as the previous case for the first and second states where (XY = 10), and the optical signal is transmitted to drop-port (DR3) as optical logic "1". Where in this state, the control input is applied (Z = 1), thus, the optical signal from MRR4 is appeared at through-port (TH6) and represents the optical logic "10000010" at output-ports "TH2-DR2-TH3-DR3-TH5-DR5-TH6-DR6". Figure 5g shows the output when the input XYZ is "110". This case, the control pulse is applied to MRR1 (X = 1), thus the input signal is transmitted to through-port (TH1). Next, the control input (Y = 1) is applied to MRR3, thus the signal from MRR1 (TH1) is through-port (TH3) to be optical logic 1. The signal from TH3 is again used as the input signal of MRR4 via input-port and appear at the drop-port (DR4). The signal is then transmitted into MRR5. For this state, no control input (Z = 0) is applied, thus, the optical signal is appeared at drop-port (DR5) and represents the optical logic "00100100" at output-ports "TH2-DR2-TH3-DR3-TH5-DR5-TH6-DR6". Lastly, Fig. 5h shows the output when the input XYZ is "111". This case is the same as the previous case for the first and second states where (XY = 11), and the optical signal is transmitted to through-port (TH3) as optical logic "1". Where in this state, control input (Z = 1) is applied to MRR5, thus, the optical signal from MRR4 (DR4) is appeared at through-port (TH5) and represents the optical logic "00101000" at output-ports "TH2-DR2-TH3-DR3-TH5-DR5-TH6-DR6". In Table 3, we conclude the optical logic of all-optical ALU circuit obtained from output-ports TH2, DR2, TH3, DR3, TH5, DR5, TH6, DR6 of MRR2, MRR3, MRR5, MRR6, respectively. Where the output signal can be used to perform all-optical full-adder/half adder. The arithmetic operation can be done by using beam-splitter and beam combiner to split and combine optical output intensity such as the SUM = TH5 + DR6; CAR = TH3 + TH6 for summation and carry out of full-addition, DIF = TH5 + DR6; BOR = TH2 + TH5 for difference and borrow of full-subtraction, respectively. This output logic can be implemented in other arithmetic and logic operation such as XOR gate, XNOR gate, increment and decrement.

5 Discussion

Light travelling with the nonlinear microring material has the advantage of the short output pulse generation, which is the objective of this work. In which the ultrashort pulses can give

the ultra-fast transmission. The soliton equation is required to appear along with the result. Because of the soliton pulse will be affected by the larger nonlinear effect due to the Kerr effect. The single soliton pulse is sliced to be multi-peaks, from which the single peak is shorter in time. The device scale is within the range of the current fabrication technology ability. The controlled input wavelength is 1.55 μm, which is the required to match with the input soliton for switching identification. The initial estimated propagation time can be calculated by $\tau_{pr} = OPLn_{eff}/c$, where OPL is the optical path length inside 4 micro rings (MRR1, MRR2, MRR4, MRR5) that the light propagating from input-port of MRR1 to drop-port DR5 of MRR5 (Fig. 2) while the length of the waveguide connected between 4 micro rings is neglected, n_{eff} is the effective refractive index of InGaAsP/InP (3.34), and c is the speed of light. Hence, $\tau_{pr} = (4 \times 2\pi r)n_{eff}/c \approx 4.2$ ps. The estimated operational speed of the circuit is 40 Gbps. It is higher compared to MZI (10 Gbps) and TOAD (11.11 Gbps) technologies. The coupling coefficient (κ) indicates the energy level induced into the cross-waveguide at the coupling length. In practice, this coefficient can be adjusted by adjusting the gap between input-waveguide and a ring resonator. The sentence just above Eq. (7) is attempted to explain that the dark and bright soliton pulses represent the input signals and the control signal as logic '0' and logic '1', respectively. The input signal is input at the input-port while the control signal is input at the add-port. In Fig. 2, the signals from DR2 (red line) and TH3 (green line) can either be the same or different depended on the control signals (X, Y), i.e., when both control signals X and Y are not applied into MRR1 and MRR2, the most signal power from input-port is transmitted to DR2 while the signal at TH3 is the rest of input-power. In other words, when both control signals X and Y are applied into MRR1 and MRR3, the most signal power from input-port is transmitted to TH3 while the signal at DR2 is the rest of input-power. Nevertheless, both signals from DR2 and TH3 are combined and used as the input signal of MRR4, while the control signal of MRR4 is the signal from the combination of TH2 and DR3 (blue lines). This control signal can be manipulated by using additional Erbium-doped fiber amplifiers (EDFA). In experimentally, it is a soliton pulse, in which the high-level signal is maintained due to the soliton pulse property called the self-phase modulation. The controlled input wavelength is 1.55 μm, which is the required to match with the input soliton for switching identification. The required power is 2.25 mW in order to make the required switching device active. In this design, all devices are available by the current fabrication technology. The beam splitter and combiner can be replaced by the optical coupler, and a ring resonator with a small radius of 1.50 μm is already fabricated (Xu et al.

Table 4 The advantages of the proposed design compare to other designs

Devices	Advantages	Disadvantages
Mach–Zehnder interferometer (MZI)	Simple structure	Using signal optical analyzer(SOA)
	Easy to operate	Large size
		Low bitrate ($\sim$ 10 Gbps)
		Difficulty in integration with very large scale integrated optics (VLSIO)
Terahertz optical asymmetric demultiplexer (TOAD)	Simple structure	Using SOA
	Easy to operate	Large size
	No additional pumping signal	Low bitrate ($\sim$ 11.11 Gbps)
		Difficulty in integration with very large scale integrated optics(VLSIO)
Microring resonator (MRR)	Small size	Requires additional erbium doped fiber amplifier, (EDFA) to manipulate the control signal
	Simple structure	
	Easy to operate	
	High bitrate ($\sim$ 40 Gbps)	
	Facility in photonic integration	

2008). The compared table of the different devices is given in Table 4.

6 Conclusion

We have proposed the design circuit of the ALU that can be used to perform the two arithmetic operations which are full-addition and full-subtraction using the semiconductor (*InGaAsP/InP*) microring resonator circuits. By using the bright soliton input signal, the operation can be successfully achieved by dark-bright soliton conversion within microring resonator, which can be used to represent optical logic NOT gate (optical switching). This dark-bright soliton conversion can be controlled, where the high-security communication in long distance using such concept has been reported and confirmed (Amiri et al. 2012; Phatharaworamet et al. 2010). The simulation shows that the ultrafast-optical switching time of ($\tau_{sw} = 0.114$ ps), an on–off ratio of $\sim$ 47.99 dB and propagation time of $\sim$ 4.2 ps are obtained. This design circuit is also the small in physical size, which is flexible in order to demonstrate in the larger amount of bits processing and considering for experimentation and fabrication.

References

Amiri IS, Babakhani S, Vahedi GR, Ali J, Yupapin PP (2012) Dark-bright solitons conversion system for secured and long distance optical communication. IOSR J Appl Phys 2(1):43–48

Amiri IS, Ariannejad MM, Ghasemi M, Ahmad H (2017) Transmission performances of solitons in optical wired link. Appl Comput Inform 13(1):92–99

Chattopadhyay T (2012) Terahertz optical asymmetric demultiplexer (TOAD) based half-adder and using it to design all-optical flip-flop. Optik Int J Light Electron Opt 123:1961–1964

Dai B, Shimizu S, Wang X, Wada N (2013) Simultaneous all-optical half-adder and half-subtracter based on two semiconductor optical amplifiers. IEEE Photonics Technol Lett 25(1):91–93

Donzella V, Sherwali A, Flueckiger J, Grist S, Fard S, Chrostowski L (2015) Design and fabrication of SOI micro-ring resonators based on sub-wavelength grating waveguides. Opt Express 23:4791–4803

Garai SK (2011) A novel all-optical frequency-encoded method to develop arithmetic and logic unit (ALU) using semiconductor optical amplifiers. Lightwave Technol 29(23):3506–3514

Gayen DK, Chattopadhyay T (2013) Designing of optimized all-optical half adder circuit using single quantum-dot semiconductor optical amplifier assisted Mach–Zehnder interferometer. J Lightwave Technol 31(12):2029–2035

Gayen DK, Bhattachryya A, Chattopadhyay T, Roy JN (2012) Ultrafast all-optical half adder using quantum-dot semiconductor optical amplifier-based Mach–Zehnder interferometer. J Lightwave Technol 30(21):3387–3393

Godbole A, Dali PP, Janyani V, Tanabe T, Singh G (2016) All optical scalable logic gates using Si_3N_4 microring resonators. IEEE J Sel Top Quantum Electron 22(6):326–333

Hwang IK, Kim MK, Lee YH (2007) All-optical switching in InGaAsP–InP photonic crystal resonator coupled with micro-fiber. IEEE Photonics Technol Lett 19(19):1535–1537

Kaur S, Kaler R, Kamal T (2015) All-optical binary full adder using logic operations based on the nonlinear properties of a semiconductor optical amplifier. J Opt Soc Korea 19:222–227

Kumar A (2016) Application of micro-ring resonator as high speed optical gray code converter. Opt Quantum Electron 48:460

Kumar S, Kumar Raghuwanshi S, Rahman BMA (2015) Design of universal shift register based on an electro-optic effect of $LiNbO_3$ in Mach–Zehnder interferometer for high-speed communication. Opt Quantum Electron 47:3509

Madani A, Azarinia H, Latifi H (2013) Design and fabrication of a polymer microring resonator with novel optical material at

add/drop geometry using laser beam direct write lithography technique. Int J Light Electron Opt 124(14):1746–1748

Mehdizadeh FMS, Alipour-Banaei H (2017) Proposal for 4–2 optical encoder based on photonic crystals. IET Optoelectron 11(1):29–35

Mookherjea S, Schneider MA (2008) The nonlinear microring add-drop filter. Opt Express 16:15130–15136

Phatharaworamet T, Teeka C, Jomtarak R, Mitatha S, Yupapin PP (2010) Random binary code generation using dark-bright soliton conversion control within a Panda-ring resonator. J Lightwave Technol 28(19):2804–2809

Raj A, Bhambri K, Gupta N (2014) Realization of all-optical full adder by utilizing DM soliton pulses. Int J Comput Appl 96(19):13–16

Rakshit JK, Chattopadhyay T, Roy JN (2013) Design of ring resonator-based all-optical switch for logic and arithmetic operations—a theoretical study. Int J Light Electron Opt 124(23):6048–6057

Rakshit JK, Roy JN, Chattopadhyay T (2014) A theoretical study of all optical clocked D flip-flop using single microring resonator. J Comput Electron 13:278

Seifert S, Runge P (2016) Revised refractive index and absorption of In1-xGaxAsyP1-y lattice-matched to InP in transparent and absorption IR-region. Opt Mater Express 6:629–639

Stanley AI, James E, Nweke FU (2015) The use of SOA-based Mach–Zehnder interferometer in designing/implementing all-optical integrated full adder-subtractor and demultiplexer. Indian J Eng Mater Sci 6(1):40–44

Teeka C, Chaiyachet P, Yupapin PP (2009) Soliton collision management in a microring resonator system. Phys Proc 2(1):67–73

Teeka C, Jalil MA, Yupapin PP, Ali J (2010) Novel tunable dynamic tweezers using dark-bright soliton collision control in an optical add/drop filter. IEEE Trans Nanobiosci 9(4):258–262

Theresal T, Sathish K, Aswinkumar R (2015) A new design of optical reversible adder and subtractor using MZI. Int J Sci Res Publ 5(4):1–6

Thongmee S, Yupapin PP (2011) All optical half adder/subtractor using dark-bright soliton conversion control. Proc Eng 8:217–222

Tian Y, Zhao Y, Chen W, Guo A, Li D, Zhao G, Liu Z, Xiao H, Liu G, Yang J (2015) Electro-optic directed XOR logic circuits based on parallel-cascaded micro-ring resonators. Opt Express 23:26342–26355

Wang W, Chu ST, Little BE, Pasquazi A, Wang Y, Wang L, Zhang W, Wang L, Hu X, Wang G, Hu H, Su Y, Li F, Liu Y, Zhao W (2016) Dual-pump Kerr micro-cavity optical frequency comb with varying FSR spacing. Sci Rep 6:28501

Xu Q, Fattal D, Beausoleil R (2008) Silicon microring resonators with 1.5-μm radius. Opt Express 16:4309–4315

Yan S, Li M, Luo L, Ma K, Xue C, Zhang W (2014) Optimisation design of coupling region based on SOI microring resonator. Micromachines 6(1):151–159